BIOCHEMISTRY
including biophysical chemistry & molecular biology

Article

pubs.acs.org/biochemistry

A Predicted Structure for the PixD−PixE Complex Determined by Homology Modeling, Docking Simulations, and a Mutagenesis Study

Shukun Ren,[†] Ryoichi Sato,[‡] Koji Hasegawa,[§] Hiroyuki Ohta,[†] and Shinji Masuda*[,†,∥]

[†]Center for Biological Resources and Informatics, Tokyo Institute of Technology, Yokohama 226-8501, Japan

[‡]Graduate School of Bioscience and Biotechnology, Tokyo Institute of Technology, Yokohama 226-8501, Japan

[§]Advancesoft Corporation, Akasaka, Tokyo 107-0052, Japan

[∥]PRESTO, Japan Science and Technology Agency, Saitama 332-0012, Japan

Supporting Information

ABSTRACT: PixD is a blue light-using flavin (BLUF) photoreceptor that controls phototaxis in the cyanobacterium *Synechocystis* sp. PCC6803. PixD interacts with the response regulator-like protein PixE in a light-dependent manner, and this interaction is critical for light signal transduction in vivo. However, the structure of the PixD−PixE complex has not been determined. To improve our understanding of how PixD transmits its captured light signal to PixE, we used blue-native polyacrylamide gel electrophoresis to characterize the molecular mass of a recombinant PixD−PixE complex purified from *Escherichia coli* and found it to be 342 kDa, suggesting that the complex contains 10 PixD and 4 PixE monomers. The stoichiometry of the complex was confirmed by Western blotting. Specifically, three intermediate states, $PixD_{10}$−$PixE_1$, $PixD_{10}$−$PixE_2$, and $PixD_{10}$−$PixE_3$, were detected. The apparent dissociation constant for PixE and PixD is ∼5 μM. A docking simulation was performed using a modeled PixE structure and the $PixD_{10}$ crystal structure. The docking simulation showed how the molecules in the $PixD_{10}$−$PixE_4$ structure interact. To verify the accuracy of the docked model, a site-directed mutagenesis study was performed in which Arg80 of PixE, which appears to be capable of interacting electrostatically with Asp135 of PixD in the predicted structure, was shown to be critical for complex formation as mutation of PixE Arg80 to Asp or Ala prevented PixD−PixE complex formation. This study provides a structural basis for future investigations of the light signal transduction mechanism involving PixD and PixE.

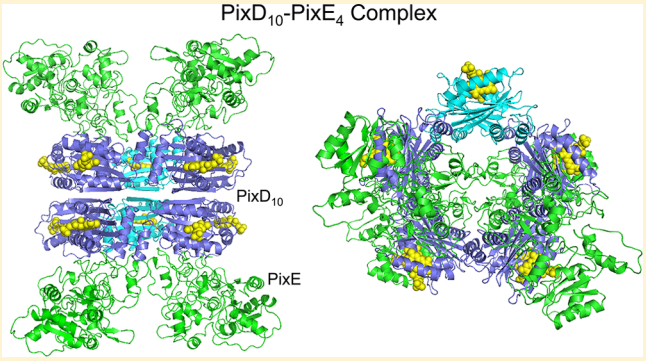

Most organisms respond to the quality and quantity of environmental light. To do so, organisms produce several types of photoreceptor-type proteins that bind chromophores that absorb light of different wavelengths and thereby control various physiological functions. Blue light-using flavin (BLUF) proteins, which are found in many bacteria and some algae, make up a class of blue light-sensing photoreceptors that contain a flavin chromophore.[1,2] PixD, a BLUF protein found in two species of cyanobacteria, *Synechocystis* sp. PCC6803 and *Thermosynechococcus elongates* BP1,[3−5] is a single-BLUF domain protein with a molecular mass of 17 kDa. A study that used a yeast two-hybrid system suggested that *Synechocystis* PixD interacts with the response regulator-like protein PixE.[4,6] Biochemical and genetic studies confirmed the physiological relevance of the PixD−PixE interaction,[7−9] which showed that although PixD and PixE mostly exist as dimers and monomers in solution, respectively, the two proteins can form a large oligomeric complex (∼370 kDa). Light excitation of the PixD−PixE complex disassembles the complex into PixD dimers and PixE monomers. A genetic study indicated that formation of the PixD−PixE complex is essential for positive phototaxis in *Synechocystis*.[7]

PixD crystal structures have been determined.[5,10] The crystallographic asymmetric unit contains a PixD decamer ($PixD_{10}$) formed by two rings containing five monomers that are stacked face to face. Using the $PixD_{10}$ structure as a guide, the PixD−PixE complex was suggested to consist of 10 PixD and 5 PixE molecules ($PixE_{10}$−$PixE_5$),[8] although the stoichiometry was not experimentally verified. In addition, the PixE structure and the structural features of the PixD−PixE complex remain unknown.

For the study reported here, the molecular mass of the PixD−PixE complex was determined by blue-native (BN) polyacrylamide gel electrophoresis (PAGE).[11] We also performed docking simulations using the crystal structure of the PixD decamer and a modeled PixE structure. The results suggest that $PixD_{10}$ interacts with four PixE monomers. A site-directed mutagenesis study provided additional evidence that

Received: July 26, 2012
Revised: December 27, 2012
Published: January 25, 2013

dx.doi.org/10.1021/bi301004v | *Biochemistry* 2013, 52, 1272−1279

the two proteins interact as suggested by the docking simulation.

MATERIALS AND METHODS

Protein Purification. PixD and PixE were co-expressed in *Escherichia coli*. For this purpose, the PixE coding region was amplified via PCR using pETslr1693 plasmid DNA[7] as the template, the forward primer (5′-AGGAGATATACCATGCATCATCATCATCATCACATGAGCAATTCAGTTTTGTCC-3′), and the reverse primer (5′-GCTCGAATTCGGATCTCAGGAGTTGGTTTTATTGGTGGG-3′). The forward primer has a hexahistidine tag sequence (underlined) upstream of the first PixE codon. Amplified DNA was cloned into the *Nco*I−*Bam*HI site of pCDFDuet-1 (Novagen) using In Fusion Cloning reagents (Clontech), and the plasmid was named pCDF-PixE.

The PixD coding region was amplified via PCR using pTYslr1694 plasmid DNA[12] as the template, the forward primer (5′-AAGGAGATATACATATGAGTTTGTACCGTTTG-3′), and the reverse primer (5′-CTTTACCAGACTCGAGTTAGAGGTCGAGGAAAAAG-3′). The amplified fragment was cloned into the *Nde*I−*Xho*I site of pCDF-PixE using In Fusion Cloning reagents, and the resulting plasmid was named pCDF-PixED.

E. coli BL21(DE3) cells were transformed with pCDF-PixED, and the resulting cells were used to co-express PixD and His_6-tagged PixE. The *E. coli* transformant was grown in LB medium with 50 mg/L streptomycin, and the two proteins were expressed by induction with isopropyl β-D-thiogalactopyranoside (1 mM, final concentration) and then cultured for >16 h at 16 °C. The expressed proteins were copurified through His-Bind resin (Merck) according to the manufacturer's instructions. The purified protein complex was dialyzed against 20 mM Tris-HCl (pH 8.0) and 200 mM NaCl.

Wild-type (WT) PixE, the Arg80 → Ala PixE mutant (R80A), the Arg80 → Asp PixE mutant (R80D), and FLAG-tagged PixE were expressed in *E. coli* as described below. PixE coding regions were amplified via PCR using pETslr1693 plasmid DNA[7] as the template, and one of two primer pairs: the forward primer (5′-AGAATGCTGGTCATATGAGCAATTCAGTTTTGTCC-3′) and the reverse primer (5′-CGGGCTCGAGGAATTCTCAGGAGTTGGTTTTATTGGTGGG-3′) for WT PixE or the same forward primer and the reverse primer (5′-CGGGCTCGAGGAATTCTCACTTATCATCATCATCCTTATAATCGGAGTTGGTTTTATTGGTGGG-3′) for FLAG-tagged PixE (the FLAG tag sequence is underlined). The amplified DNAs for WT PixE and FLAG-tagged PixE were separately cloned into the *Nde*I−*Eco*RI site of pTYB12 (New England Biolabs) using In Fusion Cloning reagents, and the resulting plasmids were named pTY-PixE and pTY-PixE-FLAG, respectively. The codon for PixE Arg80 (CGT) in pTY-PixE was replaced with that for Ala (GCT) and that for Asp (GAT) by a standard PCR mutagenesis technique, and the resulting plasmids were named pTY-PixE-R80A and pTY-PixE-R80D, respectively. These four plasmids, pTY-PixE, pTY-PixE-FLAG, pTY-PixE-R80A, and pTY-PixE-R80D, were separately transferred into *E. coli* BL21(DE3) cells, and the cells were used to express intein-tagged WT PixE, FLAG-tagged PixE, R80A mutant PixE, and R80D mutant PixE, respectively. The transfected *E. coli* cells were grown in LB medium with 100 mg/L ampicillin, and the proteins were expressed by induction with isopropyl β-D-thiogalactopyranoside (1 mM, final concentration) and then cultured for >16 h at 16 °C. The expressed proteins were purified by chitin affinity chromatography (New England Biolabs) according to the manufacturer's instructions. The intein tag was removed by incubation with a buffer containing 20 mM Tris-HCl (pH 8.0), 200 mM NaCl, and 200 mM dithiothreitol. The purified proteins were dialyzed against 20 mM Tris-HCl (pH 8.0) and 200 mM NaCl. PixD was purified as described previously.[12]

BN-PAGE, Western Blotting, and Kinetic Analysis. BN-PAGE was performed using the NativePAGE Novex Bis-Tris Gel system (Invitrogen). 2D sodium dodecyl sulfate (SDS)−PAGE was conducted with a 16% (w/v) polyacrylamide gel. For Western blotting, proteins electrophoresed through a BN-PAGE gel were electroblotted onto a polyvinylidene fluoride membrane. Protein bands that reacted with antibody to FLAG M2 (Sigma-Aldrich) were detected by SuperSignal West Femto reagents (Thermo Scientific). LumiCube (Liponics Inc.) was used to quantify band intensities. The kinetic parameters for the PixD−PixE complex intermediate formation were determined using the following equations:

$$v_n = k_n[\mathrm{PixD}_{10}{-}\mathrm{PixE}_{n-1}][\mathrm{PixE}] \quad (1)$$

$$v_{-n} = k_{-n}[\mathrm{PixD}_{10}{-}\mathrm{PixE}_{n}] \quad (2)$$

where n is the number of one of the four reaction steps shown in Figure 4A, v is the initial rate, k is the rate constant for each reaction step, $[\mathrm{PixD}_{10}{-}\mathrm{PixE}_{n-1}]$ (or $[\mathrm{PixD}_{10}{-}\mathrm{PixE}_{n}]$) is the concentration of each PixD−PixE intermediate, and [PixE] is the PixE concentration. Data were fitted, and apparent rate constants for each PixD−PixE complex intermediate formation were determined using a homemade computer program. The program was run at various PixE concentrations with a fixed PixD concentration of 54 μM.

PixE Homology Modeling. The amino acid sequence of PixE was obtained from the DNA Data Bank of Japan (entry YP_005651766.1). A full-length, homology-modeled PixE (380 residues) was constructed at the SAM-T08 web server, which predicted by multiple-sequence alignments and hidden Markov models using putative local structural fragments from a large number of template proteins.[13−15] For PixE modeling, the major template proteins used were bacterial response regulators (best 20 defined as those with the smallest E values; PDB entries 3LUF, 3N0R, 3GT7, 1QKK, 3KHT, 3RQI, 2ZQT, 2QZJ, 3CG4, 1ZGZ, 1KGS, 3F6P, 3HV2, 2OQR, 1DBW, 2ZAY, 1MVO, 3CFY, 1SRR, and 1ZH2). To relax the structure of the initial PixE model, we subjected the model to a molecular dynamics (MD) simulation by NAMD version 2.8.[16] Hydrogen atoms for the PixE model were added by assuming neutral pH so that Arg/Lys and Asp/Glu residues were positively and negatively charged, respectively, His was uncharged and protonated at Nτ, and all other residues were uncharged. The model was solvated in a 100 Å × 120 Å × 120 Å box containing 35018 TIP3P water molecules, 334 Na^+ ions, and 337 Cl^- ions to neutralize the system. The MD calculation was performed using the OPLS force field combined with a periodic boundary condition that used the particle mesh Ewald approach and an *NPT* ensemble that used the Langevin dynamics and piston to fix the temperature (300 K) and pressure (1 atm). After energy minimization (30000 conjugate gradient steps), thermal equilibration (800 ps) from 10 to 300 K was performed in steps of 10 K. The MD simulation at 300 K was stopped at 10 ns, by which time the total potential energy of the system had equilibrated. The 10 ns, 300 K trajectory structure was cooled to 10 K in steps of 10 K (800 ps) and then energy minimized to

dx.doi.org/10.1021/bi301004v | *Biochemistry* 2013, 52, 1272−1279

yield the final PixE model. The quality of the model was assessed using RAMPAGE[17] to confirm that allowed amino acid conformations existed.

Docking of PixE into the PixD Decamer. The X-ray structure of the 1.8 Å resolution, two-layer pentameric ring $PixD_{10}$ (PDB entry 2HFN) was used for docking. Water molecules or ions included in the PixD structure and PixE model were removed before docking. Then one PixE was docked onto $PixD_{10}$ by ZDOCK,[18] after which a second PixE was docked onto the best PixE–$PixD_5$ substructure using ring symmetry as the guide. A third PixE could not be docked onto the $PixE_2$–$PixD_5$ structure because of steric interference between the third PixE and a docked PixE. Instead, the $PixE_4$–$PixD_{10}$ structure was constructed by stacking two $PixE_2$–$PixD_5$ complexes using PixD decamer symmetry as the guide.

RESULTS

BN-PAGE. We first determined the molecular mass of the PixD–PixE complex using BN-PAGE. A previous study indicated that PixD and PixE, heterologously co-expressed in *E. coli*, formed a complex that could be isolated by affinity purification.[8] We isolated the PixD–PixE complex by the aforementioned method and recovered a PixD–PixE complex for which the proteins were >95% pure according to their migration positions in a denaturing polyacrylamide gel (Figure 1A). The isolated complex was also subjected to BN-PAGE (Figure 1B), and the gel contained Coomassie blue-stained bands with molecular masses of 720, 342, and 172 kDa (Figure 1C).

Two-dimensional BN-PAGE and SDS–PAGE was then performed to characterize the protein compositions of the three bands (Figure 1D). The calculated molecular masses of PixD and PixE, deduced from their amino acid sequences, are 17 and 43 kDa, respectively. The 2D gel shows that the 172 kDa band contains only PixD, and the 342 kDa band contains both PixD and PixE. However, the 720 kDa band contains an unidentified protein. Given the calculated molecular mass of PixD, the 172 kDa band could correspond to the PixD decamer. The molecular mass of the 342 kDa species is that expected for the sum of the molecular masses of a PixD decamer (172 kDa) and four PixE monomers, i.e., $PixD_{10}$–$PixE_4$.

Isolated PixD and PixE were also subjected to BN-PAGE. Purified PixD migrated as three bands with molecular masses of 240, 172, and 35 kDa (bands 1–3, respectively, in Figure 2A, lane 1). After purified PixE had been mixed with PixD, bands corresponding to 342 and 70 kDa were present in a BN-PAGE gel (bands x and y, respectively, in Figure 2A), and their relative intensities depended on the amount of PixE added (lanes 2–4). 2D BN-PAGE and SDS–PAGE of the proteins in lane 4 of Figure 2A (Figure 2B) indicated that band 2 contained only PixD, band 3 contained PixD and PixE, and band 1 contained an unidentified ~50 kDa protein that was slightly present in the purified PixD fraction (Figure 1 of the Supporting Information). Given the molecular mass of PixD (17 kDa), the 172 and 35 kDa bands (bands 2 and 3, respectively) correspond to the PixD decamer and dimer, respectively, indicating that PixD equilibrates between a dimer and a decamer. Because PixE is a monomer in solution[8] and its molecular mass is 43 kDa, monomeric PixE and dimeric PixD would migrate at approximately the same rate in BN-PAGE (band 3). The 2D BN-PAGE and SDS–PAGE study also indicated that the 342 kDa band (band x) contains both PixD and PixE (red asterisks in Figure 2B), which would correspond to the $PixD_{10}$–$PixE_4$ structure. The 70 kDa band (band y) contains an unknown protein that was slightly present in both PixD and PixE preparations (Figure 1 of the Supporting Information). The intensities of the Coomassie blue-stained small and large bands for the 342 kDa species are divided by the numbers of amino acids for PixD (150 amino acids) and PixE (380 amino acids), respectively, providing a molar ratio of 2.3 ± 0.1 PixD per PixE.

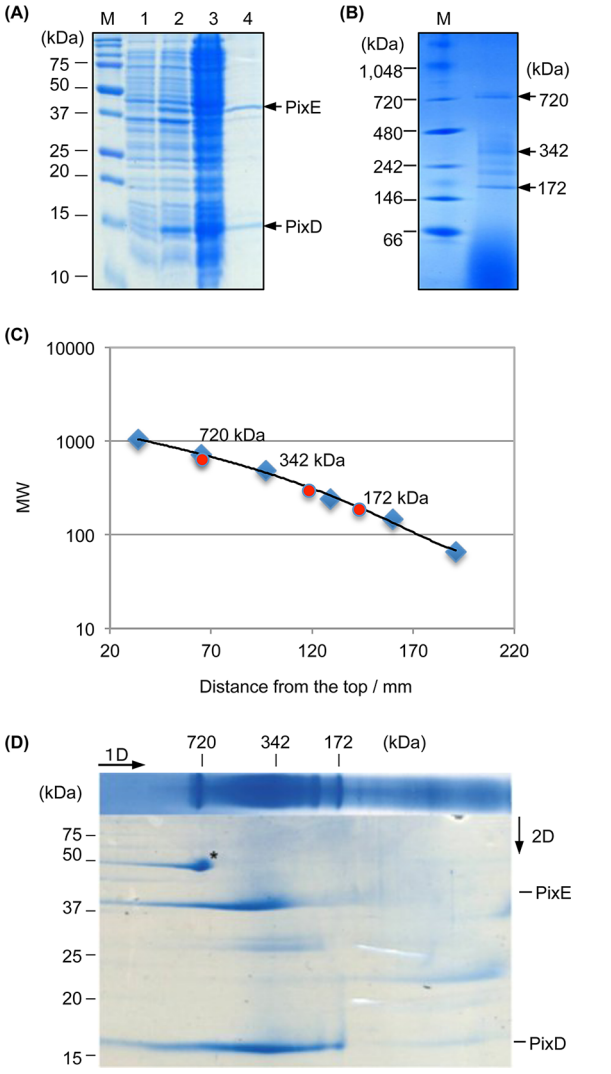

Figure 1. (A) SDS–PAGE of purified, co-expressed PixD and PixE: M, protein standards; lane 1, cell extract before induction; lane 2, cell extract after induction; lane 3, soluble fraction; lane 4, purified PixD–PixE complex. (B) BN-PAGE of the purified PixD–PixE complex. Loaded protein, 6.4 μg. (C) Calibration curve drawn using the molecular masses of standard proteins (diamonds), which are IgM pentamer (1048 kDa), apoferritin band 1 (720 kDa), apoferritin band 2 (480 kDa), B-phycoerythrin (242 kDa), lactate dehydrogenase (146 kDa), and bovine serum albumin (66 kDa). The migration positions of the three major bands shown in panel B are marked with red circles. The equation for fitting the line is $y = 0.0325x^2 - 13.551x + 1470.4$ ($R^2 = 0.9986$). (D) Two-dimensional BN-PAGE and SDS–PAGE of the PixD–PixE complex. The PixD–PixE complex (24 μg) was separated by BN-PAGE in the first dimension (1D) followed by SDS–PAGE in the second dimension (2D). An asterisk indicates an unidentified protein. Proteins were stained with Coomassie Brilliant Blue.

dx.doi.org/10.1021/bi301004v | *Biochemistry* 2013, 52, 1272–1279

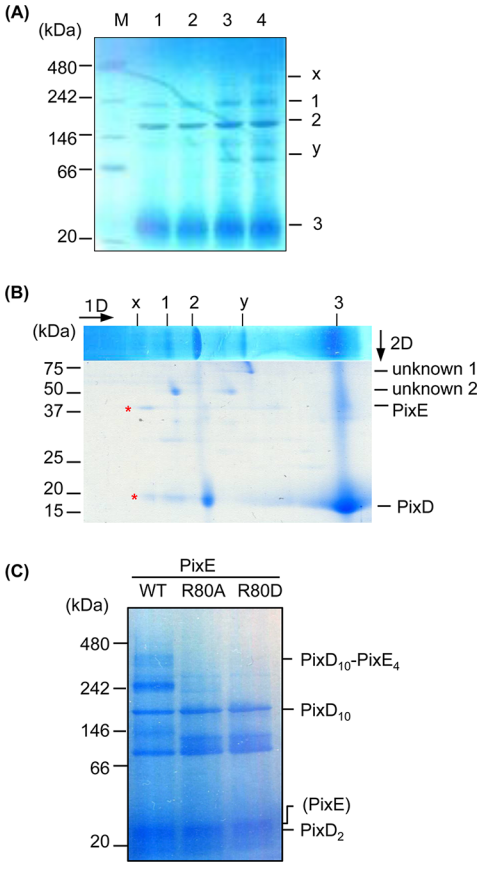

Figure 2. (A) BN-PAGE of purified PixD in the absence or presence of PixE: lane 1, only PixD (6.2 μg); lane 2, PixD (6.2 μg) and PixE (0.6 μg); lane 3, PixD (6.2 μg) and PixE (1.5 μg); lane 4, PixD (6.2 μg) and PixE (3.1 μg). (B) The proteins in lane 4 of the BN-PAGE gel shown in panel A were subjected to 2D BN-PAGE and SDS–PAGE. Bands for PixD and PixE, from band *x*, are denoted with red asterisks. (C) BN-PAGE of mixtures of purified PixD (6.2 μg) and WT PixE (8.4 μg), R80A (8.6 μg), or R80D (8.6 μg).

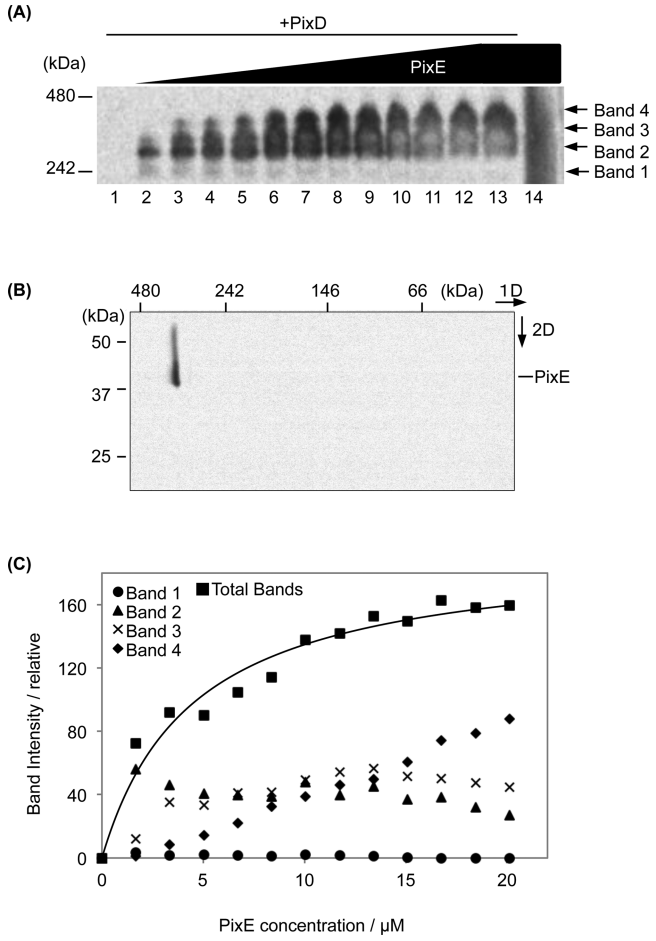

Figure 3. (A) Western blotting of purified PixD and PixE. PixD (54 μM) and different amounts of PixE (0–44 μM) were subjected to BN-PAGE followed by Western blotting. (B) The proteins in lane 13 of the BN-PAGE gel shown in panel A were subjected to 2D BN-PAGE and SDS–PAGE followed by Western blotting with an anti-FLAG antibody. (C) PixD–PixE binding curve derived from each intensity and the summed intensities of PixE per lane in the Western blot. K_d was calculated to be 4.67 ± 0.08 μM.

We next characterized PixE-dependent PixD oligomerization in more detail, using FLAG-tagged PixE and Western blotting to detect the PixD–PixE complex. Different concentrations of purified FLAG-tagged PixE (0–44 μM) were mixed with 54 μM purified PixD, and the mixtures were subjected to BN-PAGE followed by Western blotting to detect the PixD–PixE complexes using a FLAG-specific antibody. Four different PixD–PixE complexes were detected, with molecular masses of ~220, 260, 300, and 340 kDa (bands 1–4, respectively, in Figure 3A). The experimental molecular masses of bands 1–4 corresponded to the calculated molecular masses of the $PixD_{10}$–$PixE_1$ (215 kDa), $PixD_{10}$–$PixE_2$ (258 kDa), $PixD_{10}$–$PixE_3$ (301 kDa), and $PixD_{10}$–$PixE_4$ (344 kDa) structures, respectively. 2D SDS–PAGE and Western blotting of the proteins in lane 13 of Figure 3A confirmed that the FLAG-tagged PixE was highly enriched in the 340 kDa band (Figure 3B). The intensity of the four bands in each lane was plotted against the corresponding initial PixE concentration (Figure 3C). The intensities of band 1 (circles) were always low, with a highest intensity at ~2 μM PixE. The magnitudes of band 2 (triangles) were rapidly increased, which were then decreased gradually. The decrease in the magnitude of band 2 was coupled with the increase in the magnitude of band 4 (diamonds). The magnitudes of band 3 (crosses) were rather constant at >5 μM PixE. The summed intensity of the four bands in each lane was plotted against the corresponding initial PixE concentration (Figure 3C, squares) to determine the apparent K_d for PixD–PixE complex dissociation (4.67 ± 0.08 μM).

We next evaluated the kinetic data by a computer simulation. Given the four different oligomers, assigned to be $PixD_{10}$–$PixE_1$, $PixD_{10}$–$PixE_2$, $PixD_{10}$–$PixE_3$, and $PixD_{10}$–$PixE_4$, were detected (Figure 3A), we hypothesized the reaction scheme for PixD–PixE complex formation as seen in Figure 4A, where different rate constants for each reaction step (k_n or k_{-n}) were hypothesized. By a computer simulation, data points from Western blotting (Figure 3C) were fit and apparent rate constants were calculated (Figure 4B). The data were well reproduced by the simulation, where rate constants for the forward reaction, k_1–k_4, were calculated to be 2000, 55555, 296, and 1851 μM^{-1} s^{-1}, respectively, and those for the back reaction, k_{-1}–k_{-4}, were calculated to be 0.002, 0.001, 0.002, and 0.180 s^{-1}, respectively.

Homology Modeling of PixE. To gain additional insight into the PixD–PixE interaction(s), we next modeled the PixE structure. PixE contains 380 residues. We found that the PixE

dx.doi.org/10.1021/bi301004v | *Biochemistry* 2013, 52, 1272–1279

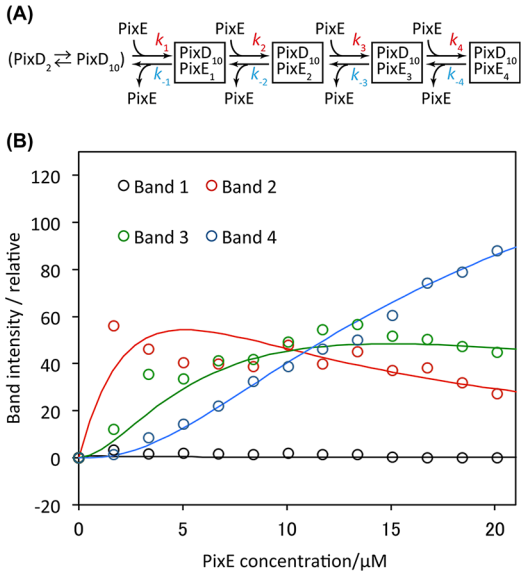

Figure 4. (A) Reaction scheme for PixD–PixE complex formation. Rate constants in each reaction step (k_n or k_{-n}) are indicated. (B) Circles are experimentally obtained data given from each band intensity of the Western blotting shown in Figure 3A, which are identical to those seen in Figure 3C. Lines are results of a computer simulation to reproduce and fit the experimental data based on eqs 1 and 2.

C-terminal region (residues 258–373) is similar in sequence to those of bacterial response regulators found in the GTOP protein structural database (http://spock.genes.nig.ac.jp/~genome/gtop.html). For example, the levels of sequence identity between PixE and *Bacillus subtilis* PhoP (PDB entry 1MVO) and PixE and *Thermotoga maritime* class I HK853 (PDB entry 3DGE) are 28.1 and 24.1%, respectively. However, because there is no homologous protein with a resolved structure for the PixE N-terminal sequence, we could not model the N-terminal region of PixE by a conventional comparative–homology modeling procedure using a structural template. The PixE structural model, including the N-terminal region, is necessary to investigate the binding of PixD to PixE, because the N-terminal region of PixE was suggested to interact with PixD.[4] Thus, we tried to use the hidden Malkov model-based protein structure prediction server SAM-T08[15] to model the putative full-length PixE structure. To the best our knowledge, SAM-T08 is the only protein modeling server (software) that can predict a reliable protein model with more than 300 amino acids, without a template protein for a targeted full-length sequence. The server can construct the protein by performing iterative searches for structural templates containing similar targeted sequence fragments and then selecting for best scored template fragments to generate a PixE conformation. The PixE model was built using structural fragments from bacterial response regulators (see Materials and Methods for additional details). Because we could not confirm the structural reliability of the obtained PixE model due to the lack of experimental structural information about PixE or other structural models using different modeling algorithms, the PixE model was subjected to the 300 K MD calculation to gain a thermally stable conformation. The final PixE model shown in Figure 2 of the Supporting Information is termed our putative PixE model.

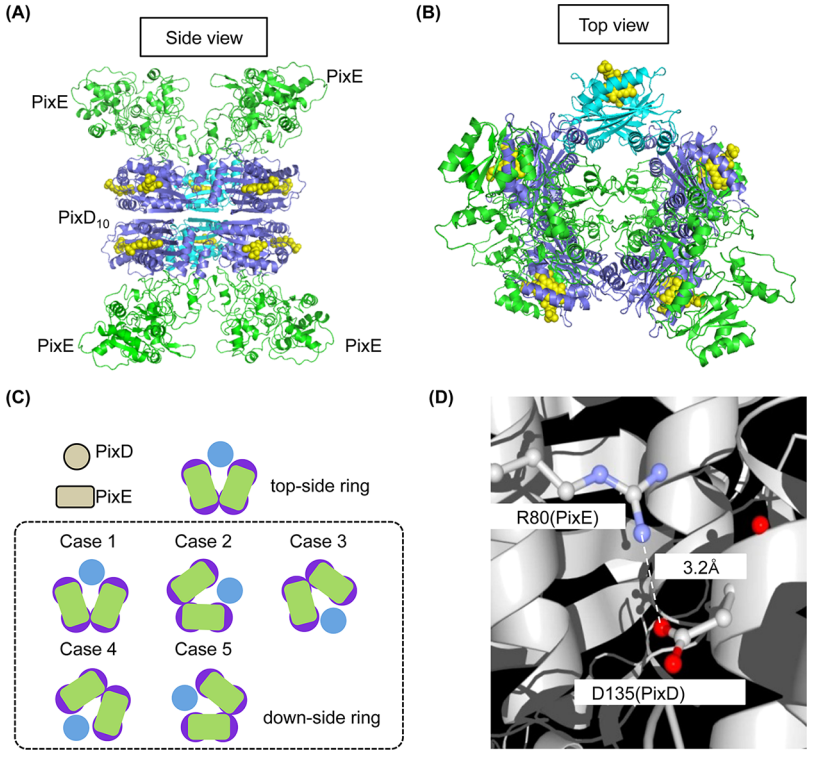

Figure 5. Docked PixD–PixE complex. (A) Side and (B) top views of the $PixD_{10}$–$PixE_4$ complex. PixE monomers are colored green, PixD monomers bound to PixE monomers purple, and PixD monomers not bound to PixE monomers blue. Flavin molecules are indicated as yellow spheres. (C) Five possible arrangements for PixE monomers in the bottom ring of the $PixD_{10}$–$PixE_4$ complex referenced to the position of PixE in the top ring. (D) Predicted salt bridge between the side chains of PixE Arg80 and PixD Asp135 in the docked structure.

dx.doi.org/10.1021/bi301004v | *Biochemistry* 2013, 52, 1272–1279

PixD−PixE Docking Simulation. We next performed a docking simulation using the PixE model and the $PixD_{10}$ crystal structure. Panels A and B of Figure 5 show the side and top views, respectively, of the best structure for the docked PixD−PixE complex. The PixE N-terminal domain interacts at the interface of two adjacent PixD monomers in the same ring. There is sufficient surface area for two PixE monomers to bind a PixD pentameric ring, indicating that four PixE-binding sites exist in $PixD_{10}$. Therefore, the molecular mass for the computationally derived PixD−PixE complex agrees with that determined by BN-PAGE. In the model, two PixD monomers (colored blue in Figure 5A,B) in a ring do not interact with PixE. Assuming that the structure of the complex is correct, five possible arrangements of PixE in the $PixD_{10}$−$PixE_4$ structure exist. Specifically, the relative locations of the two PixE monomers on one ring can be related to the two PixE monomers on the second ring by 72° rotations around the center of the PixD rings [i.e., 0°, 72°, 144°, 216°, and 288° (Figure 5C)]. Panels A and B of Figure 5 show the $PixD_{10}$−$PixE_4$ complex, with the PixE monomers from opposing PixD pentamers aligned as in case 1 (Figure 5C).

Mutational Study. In the predicted PixD−PixE structure, the side chain guanidinium nitrogen of Arg80 in PixE appears to be within ionic bonding distance of the side chain carboxyl of Asp135 in PixD (Figure 5D). Such an interaction might be important if PixE interacts with PixD as suggested by the model. To determine if an Arg80−Asp135 interaction exists, we performed BN-PAGE using R80A and R80D mutant PixE and WT PixD. The 342 kDa band corresponding to the $PixD_{10}$−$PixE_4$ complex was absent when R80A or R80D replaced WT PixE (Figure 2C), indicating that Arg80 is necessary for complex formation. An apparent ∼250 kDa band may correspond to band 2 shown in Figure 3A. No significant difference was observed in limited proteolysis patterns for WT and R80A mutant PixE (Figure 3 of the Supporting Information), suggesting that the R80A mutation does not affect the overall conformation and stability of PixE. We also attempted to characterize the interaction of the Asp135 → Ala or Asp135 → Arg PixD mutant with PixE; however, the mutant was unstable and could not be purified.

DISCUSSION

Recently, BN-PAGE has been used for protein complex isolation, native protein mass determination, and oligomeric state characterization to identify physiological protein−protein interactions.[11] Here, we applied BN-PAGE to examine PixD−PixE complex formation. Because BN-PAGE is based on a charge shift of the Coomassie-stained proteins, electrophoretic mobility patterns of each protein or protein complex depended on their physical and chemical properties, i.e., size, shape, and/or hydrophobicity.[11] However, the calibration curve defined by regression analysis of the molecular masses of different protein standards (Figure 1C) is highly accurate (adjusted $R^2 = 0.998$), which allowed us to confidently determine the molecular masses of the PixD−PixE complex. It is of note that according to the calibration curve, molecular masses of a PixD decamer and a PixD dimer were calculated to be 172 and 35 kDa, respectively (Figures 1C and 2A), which are well fit to those calculated from their amino acid sequences (170 kDa and 34 kDa, respectively), supporting the accuracy of the calculation curve. On the basis of the calculation, the molecular mass of the PixD−PixE complex, isolated from *E. coli*, is 342 kDa. This complex could also be formed in vitro by mixing isolated PixD and PixE (Figure 2A). Given the molecular mass of 342 kDa, we could assign the complex stoichiometry as 10 PixD monomers to 4 PixE monomers. The 172 kDa band in Figure 1B could be assigned to the PixD decamer and corresponds to the 172 kDa band in lane 1 of Figure 2A. Therefore, PixD and PixE most likely form the $PixD_{10}$−$PixE_4$ complex.

The molecular mass of the PixD−PixE complex determined in this study (342 kDa) differs from that suggested by a gel-filtration study (∼370 kDa) and sedimentation equilibrium analysis (∼390 kDa), which would correspond to a $PixD_{10}$−$PixE_5$ complex.[8] However, in general, the Stokes radius of a protein or protein complex can significantly affect the corresponding gel-filtration retention time with even a small Stokes radius-induced retention time error substantially affecting the calculated molecular mass. Furthermore, protein complexes exhibit a so-called reaction boundary that shows different sedimentation patterns when each free species and complex species are in fast equilibrium.[19] These types of errors may account for the differences in the stoichiometries. Notably, an isothermal titration calorimetry study[8] supports our conclusion that $PixD_{10}$ binds four PixD monomers. Specifically, the calorimetry study indicated a 2.56:1.0 PixD:PixE stoichiometry,[8] which is that expected for the $PixD_{10}$−$PixE_4$ complex (2.5 PixD per 1.0 PixE). However, it should be noted that our results and previous results were based on proteins heterologously expressed in *E. coli*. In vivo analysis of PixD and PixE in *Synechocystis* would be necessary for further investigation of complex formation.

BN-PAGE analysis of purified PixD indicated that it equilibrates between a dimer and a decamer even in the absence of PixE (Figure 2A, lane 1), although oligomeric states of dark-adapted PixD in solution have been reported to be solely dimer[8] or decamer.[9] Tanaka et al. suggested that an additional two-residue extension at the N-terminus affects the decamer formation of PixD, possibly because of steric hindrance.[9] However, this may not be the case because our construct, used in this study, has the amino acid extension. Perhaps oligomeric states of PixD could be easily affected by several environmental factors such as protein concentration, salt, and temperature, even in the dark.

A binding constant (K_a) between PixD and PixE was previously reported to be ∼5.7 μM^{-1}, which gives a dissociation constant (K_d) of ∼0.175 μM.[8] However, our BN-PAGE analysis indicated the apparent K_d for PixD−PixE complex dissociation to be ∼4.7 μM (Figure 3C). The exact origin of the difference is not known at present, and the origin should be explained in the future. However, a possible explanation of the different K_d values is that our PixE construct in this study was essentially the intact form compared to the one used in the previous study (His-tagged version). The difference that originated from the presence and absence of the His tag could affect complex formation.

We performed a docking simulation of the $PixD_{10}$ crystal structure and the PixE model to identify binding features for the PixD−PixE complex. The docking simulation indicated that a PixE monomer could be positioned between two PixD monomers in the same ring on its surface (Figure 5A,B). Additionally, on the same ring, there is sufficient surface area for a second PixE monomer to bind, indicating that, in total, four PixE monomers can bind to the PixD decamer; however, several spatial arrangements for the PixE monomers exist (Figure 5C). If such heterozygous arrangements exist, crystallization of the PixD−PixE complex should be difficult.

dx.doi.org/10.1021/bi301004v | *Biochemistry* 2013, 52, 1272−1279

Possibly, the five different arrangements have different free energies, and the PixD−PixE complex formed in vivo is enriched in the most thermally stable arrangement.

The accuracy of the PixD−PixE model is supported by our mutational study showing that the predicted ionic interaction between the side chains of Arg80 in PixE and Asp135 in PixD (Figure 5D) is required for complex formation and stability (Figure 2C). In addition, Western blotting indicated that more $PixD_{10}$−$PixE_2$ and $PixD_{10}$−$PixE_4$ complexes than $PixD_{10}$−$PixE_1$ and $PixD_{10}$−$PixE_3$ complexes exist at equilibrium (Figure 3A), suggesting that the binding of one PixE molecule to a PixD decamer cooperatively promotes the binding of a second PixE molecule to the same decamer. The kinetic analysis by a computer simulation supported the hypothesis; the apparent rate constants for the second (k_2) and fourth (k_4) PixE bindings are ∼30- and ∼6-fold higher than those for the first (k_1) and the third (k_3) PixE bindings, respectively (Figure 4). The cooperative binding of PixE to a PixD decamer may also be due to promotion of PixD decamer formation in the case of the second PixE binding.

Recently, the crystal structure of the PixD Tyr8 → Phe mutant was determined,[20] which is an asymmetric unit containing only six subunits arranged in a double-stacked semicircle such that the two PixD trimers are stacked face to face. Biochemical studies showed that the conformation of the mutant is locked in the light signaling state and cannot interact with PixE even in the dark.[7,20] Possibly, the hexamer found for the mutant represents a pseudotransition state involved in light signaling.[20] The geometry of our $PixD_{10}$−$PixE_4$ model supports this hypothesis because formation of stacked trimeric PixD semicircles that might form during dissociation of the pentameric rings would remove a PixE monomer from a PixD pentamer ring.

In the $PixD_{10}$ crystal structure, C-terminal α-helices from two PixD monomers interact with the β-sheet of the intervening PixD monomer in the same ring.[5,10] The light signal, perceived by the flavin chromophore, is transmitted to the C-terminal α-helices through a conformational change that involves the conserved Met93.[7,20−22] Perhaps this light-dependent conformational change causes the destabilization of the PixD−PixD interaction in one pentameric ring that then induces the dissociation of PixE from PixD. A PixD Met93 → Ala mutant could not form a decamer and could not interact with PixE,[7,9] supporting the aforementioned suggestion.

The PixE model appears to contain two domains (Figure 2 of the Supporting Information). Our docking simulation indicated that only its N-terminal domain interacts with the PixD decamer and that the C-terminal domain does not interact with PixD. A yeast two-hybrid study also suggested that a C-terminally truncated PixE could interact with PixD.[6]

The C-terminal domain is structurally similar to the receiver regions of certain bacterial response regulators. Figure 4 of the Supporting Information shows an alignment of the sequences in the C-terminal regions of two response regulators (PhoP and RegA) and PixE. To be activated, the response regulators must be phosphorylated by specific sensor kinases, and the two conserved aspartates and the conserved lysine (colored red in Figure 4 of the Supporting Information) may be necessary for the phosphorylation.[23] These three residues are not conserved in PixE, suggesting that PixE does not function as a response regulator. Perhaps PixE evolved from a response regulator and gained its function as the acceptor of blue light through its physical interaction with PixD without requiring a phospho-relay step. Notably, only the receiver regions are similar among the sequences of PixE, PhoP, and RegA, and no similarity exists between the DNA-binding domain sequences of the response regulators and PixE, which suggests that PixE is not a DNA-binding protein and must, therefore, pass the light signal to an unknown downstream factor(s) to control phototaxis in *Synechocystis*.

■ ASSOCIATED CONTENT

Supporting Information

SDS−PAGE analysis of purified PixD and PixE, a modeled PixE structure, limited proteolysis of PixE, and a partial amino acid sequence alignment of the C-terminus of PixE and receiver domains of response regulators. This material is available free of charge via the Internet at http://pubs.acs.org.

■ AUTHOR INFORMATION

Corresponding Author

*E-mail: shmasuda@bio.titech.ac.jp. Telephone: +81-45-924-5737. Fax: +81-45-924-5823.

Funding

Funded by JST PRESTO and The Naito Foundation.

Notes

The authors declare no competing financial interest.

■ ACKNOWLEDGMENTS

We thank Arjan Vermeulen and Carl E. Bauer (Indiana University, Bloomington, IN) for providing the method used to purify the PixD−PixE complex.

■ ABBREVIATIONS

BLUF, blue light-using flavin; BN, blue native; PAGE, polyacrylamide gel electrophoresis; PCR, polymerase chain reaction; PDB, Protein Data Bank; SDS, sodium dodecyl sulfate; 2D, two-dimensional.

■ REFERENCES

(1) Gomelsky, M., and Klug, G. (2002) BLUF: A novel FAD-binding domain involved in sensory transduction in microorganisms. *Trends Biochem. Sci. 27*, 497−500.

(2) Masuda, S. (2012) Light detection and signal transduction in the BLUF photoreceptors. *Plant Cell Physiol.*, 10.1093/pcp/pcs173.

(3) Masuda, S., and Ono, T. A. (2004) Biochemical characterization of the major adenylyl cyclase, Cya1, in the cyanobacterium *Synechocystis* sp. PCC 6803. *FEBS Lett. 577*, 255−258.

(4) Okajima, K., Yoshihara, S., Fukushima, Y., Geng, X., Katayama, M., Higashi, S., Watanabe, M., Sato, S., Tabata, S., Shibata, Y., Itoh, S., and Ikeuchi, M. (2005) Biochemical and functional characterization of BLUF-type flavin-binding proteins of two species of cyanobacteria. *J. Biochem. 137*, 741−750.

(5) Kita, A., Okajima, K., Morimoto, Y., Ikeuchi, M., and Miki, K. (2005) Structure of a cyanobacterial BLUF protein, Tll0078, containing a novel FAD-binding blue light sensor domain. *J. Mol. Biol. 349*, 1−9.

(6) Sato, S., Shimoda, Y., Muraki, A., Kohara, M., Nakamura, Y., and Tabata, S. (2007) A large-scale protein protein interaction analysis in *Synechocystis* sp. PCC6803. *DNA Res. 14*, 207−216.

(7) Masuda, S., Hasegawa, K., Ohta, H., and Ono, T. A. (2008) Crucial role in light signal transduction for the conserved Met93 of the BLUF protein PixD/Slr1694. *Plant Cell Physiol. 49*, 1600−1606.

(8) Yuan, H., and Bauer, C. E. (2008) PixE promotes dark oligomerization of the BLUF photoreceptor PixD. *Proc. Natl. Acad. Sci. U.S.A. 105*, 11715−11719.

(9) Tanaka, K., Nakasone, Y., Okajima, K., Ikeuchi, M., Tokutomi, S., and Terazima, M. (2011) Light-induced conformational change and transient dissociation reaction of the BLUF photoreceptor *Synechocystis* PixD (Slr1694). *J. Mol. Biol. 409*, 773−785.
(10) Yuan, H., Anderson, S., Masuda, S., Dragnea, V., Moffat, K., and Bauer, C. (2006) Crystal structures of the *Synechocystis* photoreceptor Slr1694 reveal distinct structural states related to signaling. *Biochemistry 45*, 12687−12694.
(11) Wittig, I., Braun, H. P., and Schagger, H. (2006) Blue native PAGE. *Nat. Protoc. 1*, 418−428.
(12) Masuda, S., Hasegawa, K., Ishii, A., and Ono, T. A. (2004) Light-induced structural changes in a putative blue-light receptor with a novel FAD binding fold sensor of blue-light using FAD (BLUF); Slr1694 of *Synechocystis* sp. PCC6803. *Biochemistry 43*, 5304−5313.
(13) Karplus, K., Barrett, C., and Hughey, R. (1998) Hidden (Markov) models for detecting remote protein homologies. *Bioinformatics 14*, 846−856.
(14) Karplus, K., Karchin, R., Draper, J., Casper, J., Mandel-Gutfreund, Y., Diekhans, M., and Hughey, R. (2003) Combining local-structure, fold-recognition, and new fold methods for protein structure prediction. *Proteins 53* (Suppl. 6), 491−496.
(15) Karplus, K. (2009) SAM-T08, HMM-based protein structure prediction. *Nucleic Acids Res. 37*, W492−W497.
(16) Phillips, J. C., Braun, R., Wang, W., Gumbart, J., Tajkhorshid, E., Villa, E., Chipot, C., Skeel, R. D., Kale, L., and Schulten, K. (2005) Scalable molecular dynamics with NAMD. *J. Comput. Chem. 26*, 1781−1802.
(17) Lovell, S. C., Davis, I. W., Arendall, W. B., III, de Bakker, P. I., Word, J. M., Prisant, M. G., Richardson, J. S., and Richardson, D. C. (2003) Structure validation by Cα geometry: ϕ,ψ and Cβ deviation. *Proteins 50*, 437−450.
(18) Wiehe, K., Pierce, B., Tong, W. W., Hwang, H., Mintseris, J., and Weng, Z. (2007) The performance of ZDOCK and ZRANK in rounds 6−11 of CAPRI. *Proteins 69*, 719−725.
(19) Dam, J., and Schuck, P. (2005) Sedimentation velocity analysis of heterogeneous protein-protein interactions: Sedimentation coefficient distributions c(s) and asymptotic boundary profiles from Gilbert-Jenkins theory. *Biophys. J. 89*, 651−666.
(20) Yuan, H., Dragnea, V., Wu, Q., Gardner, K. H., and Bauer, C. E. (2011) Mutational and structural studies of the PixD BLUF output signal that affects light-regulated interactions with PixE. *Biochemistry 50*, 6365−6375.
(21) Barends, T. R., Hartmann, E., Griese, J. J., Beitlich, T., Kirienko, N. V., Ryjenkov, D. A., Reinstein, J., Shoeman, R. L., Gomelsky, M., and Schlichting, I. (2009) Structure and mechanism of a bacterial light-regulated cyclic nucleotide phosphodiesterase. *Nature 459*, 1015−1018.
(22) Ren, S., Sawada, M., Hasegawa, K., Hayakawa, Y., Ohta, H., and Masuda, S. (2012) A PixD-PapB chimeric protein reveals the function of the BLUF domain C-terminal α-helices for light-signal transduction. *Plant Cell Physiol. 53*, 1638−1647.
(23) Lukat, G. S., Lee, B. H., Mottonen, J. M., Stock, A. M., and Stock, J. B. (1991) Roles of the highly conserved aspartate and lysine residues in the response regulator of bacterial chemotaxis. *J. Biol. Chem. 266*, 8348−8354.